

UC Irvine

UC Irvine Previously Published Works

Title

Middle mediastinal lesions: imaging findings and pathologic correlation

Permalink

<https://escholarship.org/uc/item/0ht4d641>

Journal

European Journal of Radiology, 35(1)

ISSN

0720-048X

Authors

Kim, Yookyung
Lee, Kyung Soo
Yoo, Jeong Hyun
[et al.](#)

Publication Date

2000-07-01

DOI

10.1016/s0720-048x(99)00156-4

Copyright Information

This work is made available under the terms of a Creative Commons Attribution License, available at <https://creativecommons.org/licenses/by/4.0/>

Peer reviewed

Middle mediastinal lesions: imaging findings and pathologic correlation

Yookyung Kim ^{a,*}, Kyung Soo Lee ^b, Jeong Hyun Yoo ^a, Chungsik Rhee ^a,
Heasoo Koo ^c, Joung-ho Han ^d, Myeong Im Ahn ^e

^a Department of Diagnostic Radiology, College of Medicine, Ewha Woman's University, 70, Chongno-6 ka, Chongno-gu, Seoul 110-126, South Korea

^b Department of Radiology, Samsung Medical Center, Sungkyunkwan University School of Medicine, Seoul 135-710, South Korea

^c Department of Pathology, College of Medicine, Ewha Womans University, Seoul 110-126, South Korea

^d Department of Diagnostic Pathology, Samsung Medical Center, Sungkyunkwan University School of Medicine, Seoul 135-710, South Korea

^e Department of Radiology, St. Vincent Hospital, The Catholic University of Korea, Suwon 442-060, South Korea

Received 14 September 1999; accepted 21 September 1999

Abstract

Lesions primarily involving the middle mediastinum are uncommon and include lymph node diseases, cystic lesions, neurogenic tumors, mesenchymal tumors, tumors of mediastinal organ, and other benign processes. In this article, we illustrate imaging findings of a variety of middle mediastinal lesions with pathologic correlation. © 2000 Elsevier Science Ireland Ltd. All rights reserved.

Keywords: Middle mediastinal lesions; Mediastinum CT; Mediastinum MR; Imaging findings; Pathologic correlation

1. Introduction

Although masses originating from the anterior or posterior mediastinum extending into the middle mediastinum are common, lesions originating in the middle mediastinum are less common. Lesions that primarily involve the middle mediastinum include neoplastic and non-neoplastic solid and cystic masses. Awareness of these various middle mediastinal lesions and their imaging findings may help distinguish among them. In this article, we illustrate a variety of disease processes that involve the middle mediastinum with pathologic correlation.

2. Normal anatomy

In this article, we define the middle mediastinum using Felson's classification which defines the mediasti-

nal compartments using an anatomic classification based on radiographic projection rather than anatomic dissection; therefore, the middle mediastinum is defined as space between imaginary lines, one along the posterior cardiac border and anterior aspect of the trachea and the other connecting a point on each of the thoracic vertebrae 1 cm behind its anterior margin [1].

3. Pathologic conditions

3.1. Lymph node diseases

3.1.1. Lymphoma

Although the anterior mediastinal and paratracheal nodes are the most frequently involved groups, any intrathoracic nodal group may be enlarged with lymphomatous involvement. Two or more nodal groups are usually enlarged in Hodgkin's disease, whereas only one nodal group is involved in about half the cases of non-Hodgkin's lymphoma [2] (Fig. 1). At computed tomography (CT), enlarged lymph nodes may be discrete or matted together and show minor

* Corresponding author. Tel.: +82-2-760-5144; fax: +82-2-760-5046.

E-mail address: yookkim@unitel.co.kr (Y. Kim).

enhancement after the administration of contrast. Low-attenuation areas resulting from cystic degeneration or necrosis may be seen in both Hodgkin's disease and non-Hodgkin's lymphoma [3]. At magnetic resonance (MR), signal intensity of lymphomatous involvement is usually homogeneous [4].

3.1.2. Metastasis

Mediastinal metastatic lymph node enlargement most commonly originates from bronchogenic carcinoma. Other common extrathoracic primary tumors that may

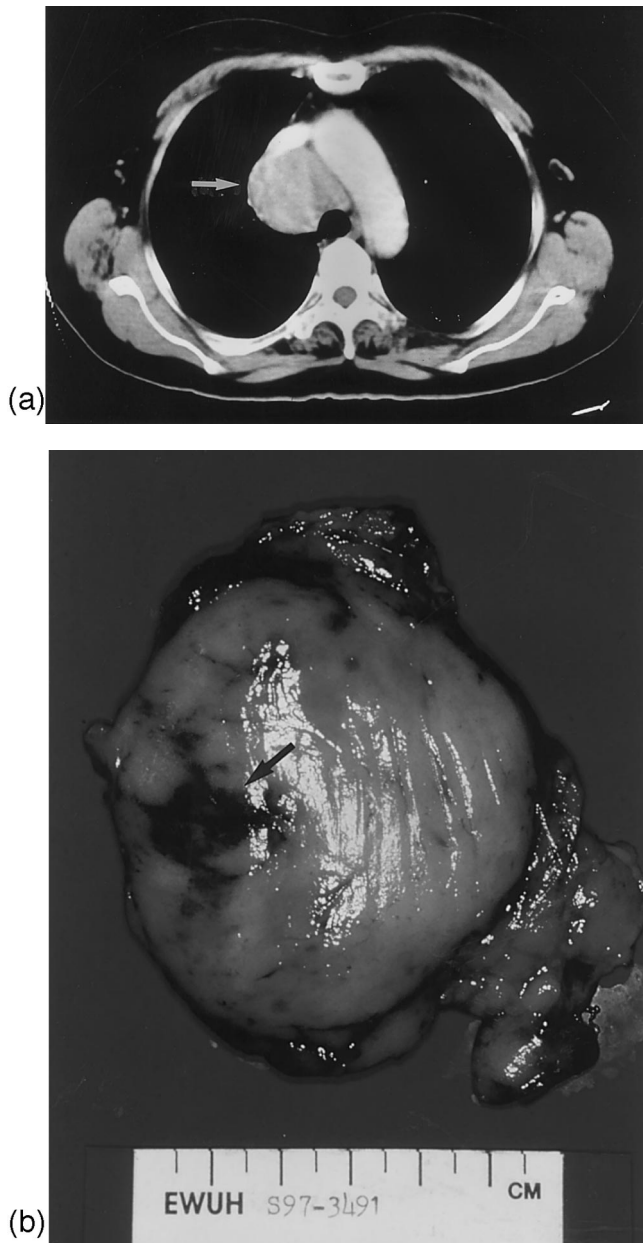


Fig. 1. Non-Hodgkin's lymphoma in a 62-year-old woman. (A) Contrast-enhanced CT scan shows homogeneous well-defined round mass (arrow) in middle mediastinum. (B) Cut surface of gross pathologic specimen shows pinkish-brown homogeneous fish-flesh appearance with focal hemorrhagic necrosis (arrow).

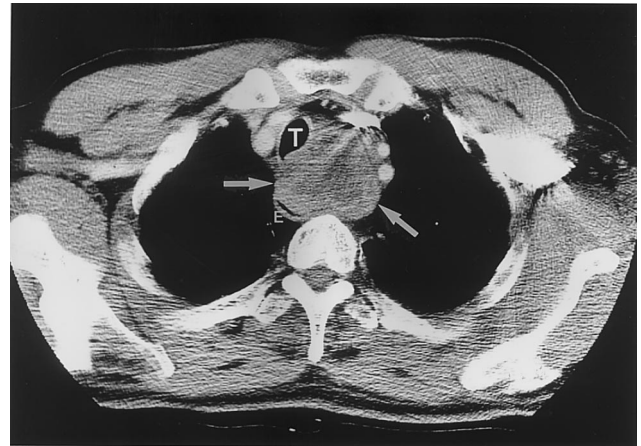


Fig. 2. Metastatic small cell lung cancer in a 60-year-old man. Contrast-enhanced CT scan shows an enlarged lymph node (arrows) with central low density, posterolateral to trachea (T). E, esophagus.



Fig. 3. Tuberculous mediastinitis in a 32-year-old man. Contrast-enhanced CT scan shows confluent lymph node enlargement (arrows) with central low attenuation in paratracheal region and AP window.

metastasize to the mediastinum include head and neck cancer, breast cancer, renal cell cancer, and melanoma. The confluence of lymph node enlargement may appear as a discrete mass (Fig. 2). At CT, lymph nodes may demonstrate central low attenuation; however, CT may demonstrate areas of increased attenuation suggesting calcification or hypervascularity [5].

3.1.3. Infections

The most frequent infections that give rise to mediastinal lymph node enlargement are tuberculosis and histoplasmosis. Tuberculous mediastinal lymph node enlargement occurs commonly in patients with primary tuberculosis and in patients with AIDS [6]. The right paratracheal region is the most common site of lymph node involvement. At CT, lymph node enlargement may demonstrate central low attenuation and peripheral rim enhancement and coalesce into poorly defined masses [7] (Fig. 3).



Fig. 4. Castleman's disease, hyaline vascular type, in a 30-year-old woman. (A) Contrast-enhanced CT scan shows enhancing right paratracheal mass (arrow). V, superior vena cava. (B) Gross specimen of mediastinal lymph node shows lobulated, solid mass with pink tan cut surface.

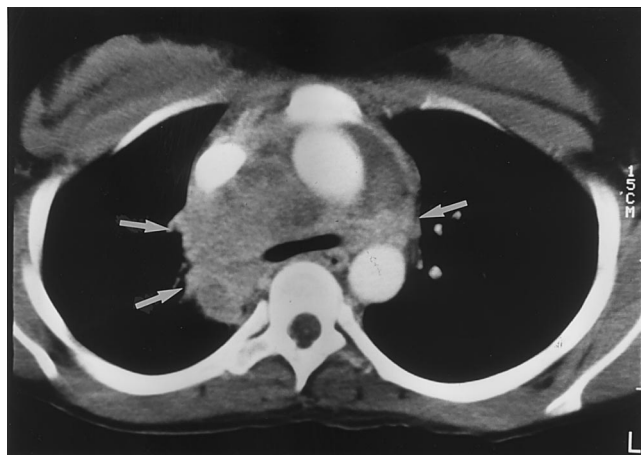


Fig. 5. Castleman's disease, plasma cell type, in a 40-year-old man. Contrast-enhanced CT scan shows poorly defined heterogeneous mass and lymph nodes (arrows) in middle mediastinum.

3.1.4. Castleman's disease

Castleman's disease represents angiofollicular lymph node hyperplasia. There are two major histopathologic variants. The hyaline vascular type (Fig. 4) is seen most frequently as an asymptomatic mass of mediastinal lymph nodes. The less frequent plasma cell variety (Fig. 5) typically appears as disseminated disease. On CT, the hyaline vascular type shows uniform enhancement and may show central coarse or punctate calcification [8].

3.2. Cystic lesions

3.2.1. Bronchogenic cyst

Bronchogenic cysts result from defective growth of the lung bud. The cysts occur most commonly within 2 cm of the carina (subcarinal; right paratracheal) but can occur anywhere in the mediastinum. They contain mucoid material of variable viscosity that causes CT attenuation to vary from that of water to soft tissue [9]. At MR, high-signal intensity is seen characteristically within cysts on T2-weighted image although variable signal intensities with different proportions of protein and/or hemorrhage in the cysts are observed on T1-weighted image [10] (Figs. 6 and 7).

3.2.2. Esophageal duplication cyst

These cystic lesions are lined by gastrointestinal tract mucosa and they are most often connected to the esophagus. The imaging features are identical to those seen with bronchogenic cysts except that the wall of the lesion may be thicker and the mass may assume a more tubular configuration [11].

3.2.3. Neurenteric cyst

These are rare lesions connected to the meninges through a midline defect in vertebral bodies. Imaging features of the cyst itself, is identical to those seen with duplication cysts, but the presence of the vertebral anomalies suggests a neurenteric cyst.

3.2.4. Pancreatic pseudocyst

Rarely, pancreatic pseudocysts extend into the mediastinum via the esophageal or aortic hiatus. CT shows a thin-walled, fluid-containing cyst within the mediastinum which may be in continuity with the pancreas and any peripancreatic fluid collections [12].

3.3. Neurogenic tumors

Rare vagal or phrenic nerve sheath tumors and paraganglioma may be situated in the middle mediastinum.

3.3.1. Nerve sheath tumors

Although almost all intrathoracic nerve sheath tumors arise from either the intercostal or the sympathetic nerves, they may arise from the phrenic or vagus

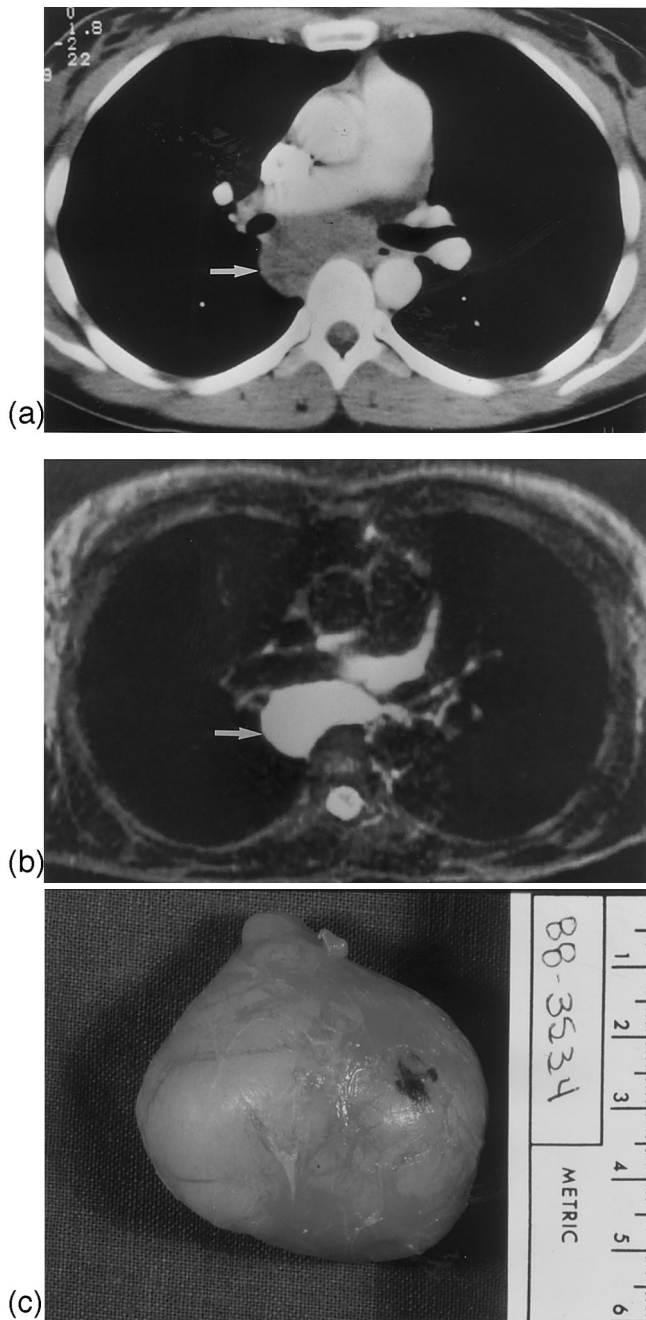


Fig. 6. Bronchogenic cyst in a 24-year-old man. (A) Contrast-enhanced CT scan shows low density cystic mass (arrow) in subcarinal area. (B) The mass (arrow) shows bright signal intensity on T2-weighted MR image. (C) Photograph of gross specimen shows a round cystic mass with smooth yellowish–brown outer surface.

nerves [13] (Fig. 8). On CT, nerve sheath tumors show heterogeneous attenuation with low attenuation area representing hypocellularity or cystic degeneration [14]. On MR, neurofibromas may appear with a so-called target pattern, with central high signal on T1-weighted image and peripheral higher signal on T2-weighted image. The target pattern corresponds pathologically to central area of nerve tissue and peripheral area of myxoid degeneration [15].

3.3.2. Paragangliomas

Mediastinal paragangliomas are rare [16] and usually located in the area of the aortic arch (aortic body tumors) in the middle mediastinum [17] (Fig. 9). Paragangliomas are usually hypervascular and show significant enhancement with administration of contrast medium on CT [18]. On MR, paragangliomas show very high signal intensity on T2-weighted image and numerous serpentine vascular channels coursing through the stroma on T2-weighted and T1-weighted image [17].

3.4. Mesenchymal tumors

3.4.1. Fatty tumors

Benign lipomas show characteristic uniform fat attenuation on CT scan. Liposarcomas show soft tissue and may or may not demonstrate fat attenuation on

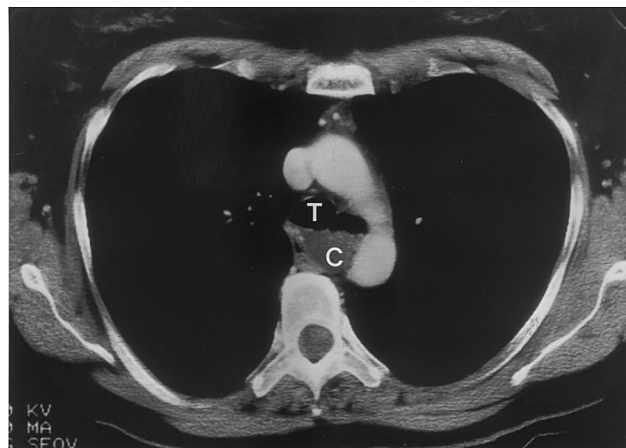


Fig. 7. Bronchogenic cyst ruptured into trachea. Contrast-enhanced CT scan shows a left paratracheal cystic mass (C) having communication with trachea (T). Air-fluid levels are observed in trachea and cystic mass.

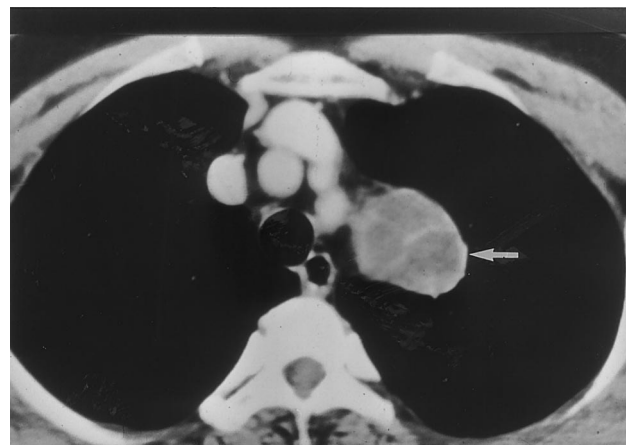


Fig. 8. Schwannoma arising from vagus nerve in a 55-year-old woman. Contrast-enhanced CT scan shows well-defined low-density mass (arrow) with septation along course of left vagus nerve.

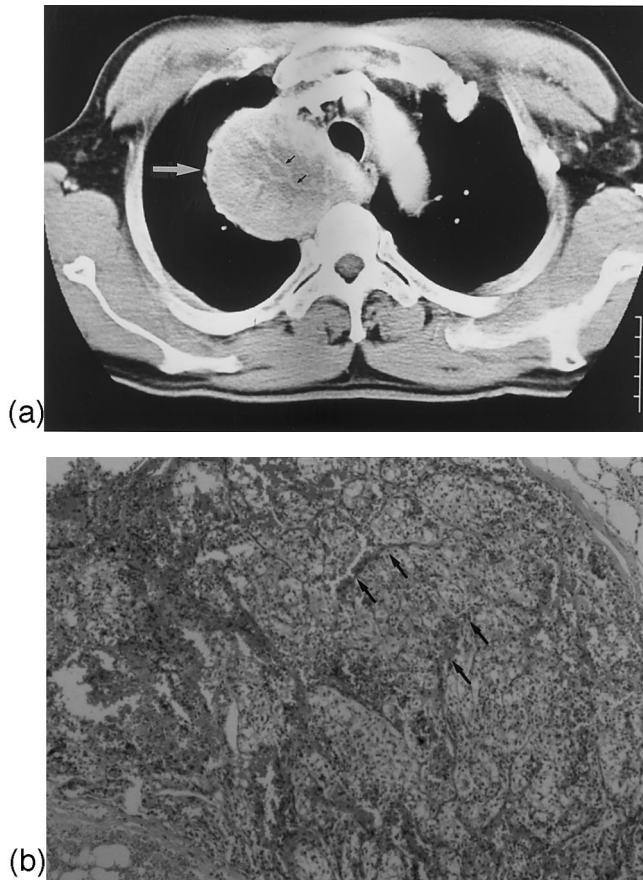


Fig. 9. Paraganglioma in a 56-year-old woman. (A) Contrast-enhanced CT scan at level of aortic arch shows highly enhanced mass (white arrow) with central low density. High-attenuation linear vascular structures (black arrows) coursing through the mass are observed. (B) Photomicrograph shows groups of tumor cells surrounded by fibrovascular septa (arrows).

CT (Fig. 10). Lipoblastoma, angioliopoma, and myelolipoma show a combination of fat and soft tissue attenuation [19].

3.4.2. Lymphangioma

Rarely lymphangiomas confined to the mediastinum are discovered in older children or adults [20]. CT shows an uni- or multilocular cystic mass with septa molding to or enveloping the adjacent structures. Vessel-like structures in the lesion are sometimes recognized on enhanced scan (Fig. 11).

3.5. Tumors of the mediastinal organs

3.5.1. Thyroid and parathyroid mass

Intrathoracic thyroid masses are almost invariably a downward extension of a thyroid mass that originates in the neck. The location of the mass is usually anterior or lateral to the trachea but may be posterior to it, forming a middle mediastinal mass [21]. On CT scan, continuity with the thyroid gland in the neck, high attenuation value on both enhanced and unenhanced

scan, calcification and low-attenuation areas in the mass are useful signs indicating a thyroid origin [22] (Fig. 12).

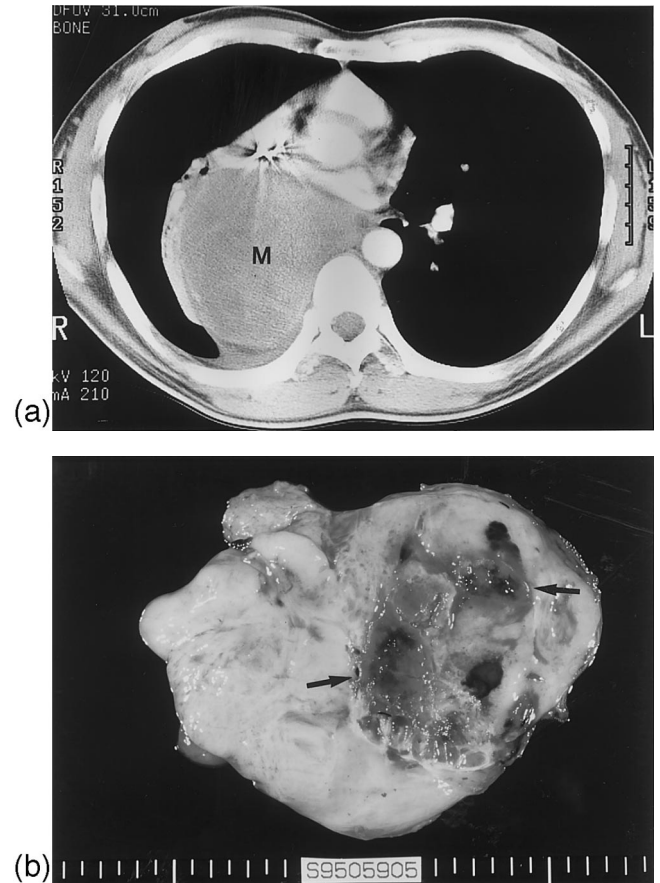


Fig. 10. Liposarcoma in a 35-year-old man. (A) Enhanced CT scan shows a large mass (M) of heterogeneous attenuation with associated pleural effusion. (B) Cut surface of gross pathologic specimen shows lobulated and encapsulated mass. It is orange–yellow and firm with areas of hemorrhage (arrows).

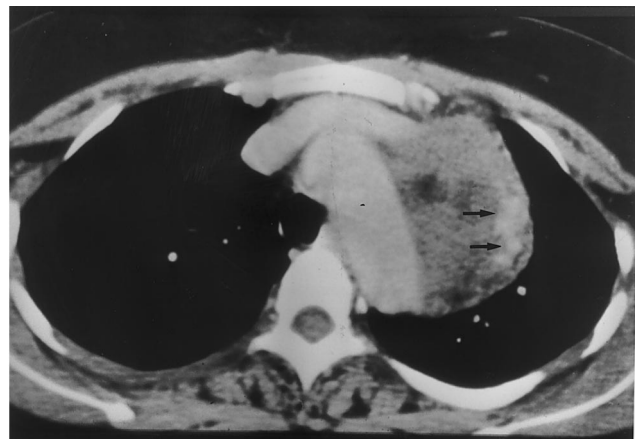


Fig. 11. Cystic lymphangioma in a 44-year-old woman. Enhanced CT scan shows mass with heterogeneous attenuation. Calcification (arrows) is also seen.

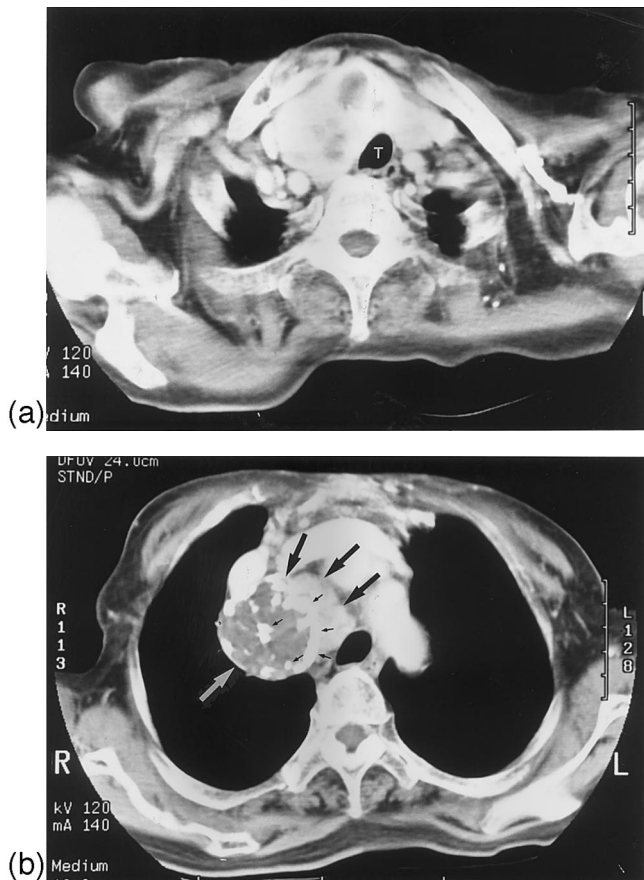


Fig. 12. Intrathoracic goiter in a 65-year-old woman. (A), (B) enhanced CT scan shows heterogeneous mass (large arrows) of mixed attenuation lateral to trachea (T). Highly enhancing portion predominates. Calcifications (small arrows) are also seen within mass. Contiguous CT scans revealed contiguity of mass with thyroid in the neck.

3.5.2. Esophageal tumor

Esophageal tumors may present as middle mediastinal masses. Anteriorly placed subserosal leiomyomas of the esophagus may present as a solid mass separating the trachea and esophagus and may confuse the origin. But this pattern may be encountered with esophageal leiomyoma and posteriorly placed intrathoracic thyroid mass but almost never is seen with other mediastinal masses [23]. CT scan shows a smooth, round, well-defined enhancing homogeneous mass inseparable from the esophagus. On MRI they show low signal intensity similar to that of skeletal muscle on T2-weighted image (Fig. 13).

3.5.3. Others

Ectopic thymoma, located entirely within the middle (Fig. 14) or posterior mediastinum is rarely reported [24]. At CT, thymoma usually shows homogeneous attenuation and uniform enhancement. Calcification and cystic change are common [25].

3.6. Benign diseases without discrete mass

3.6.1. Mediastinitis and abscess

The most common causes of mediastinitis are esophageal perforation and postoperative infection following median sternotomy. Mediastinal widening, pneumomediastinum, obliteration of mediastinal fat planes, localized fluid collections and abscess, are seen

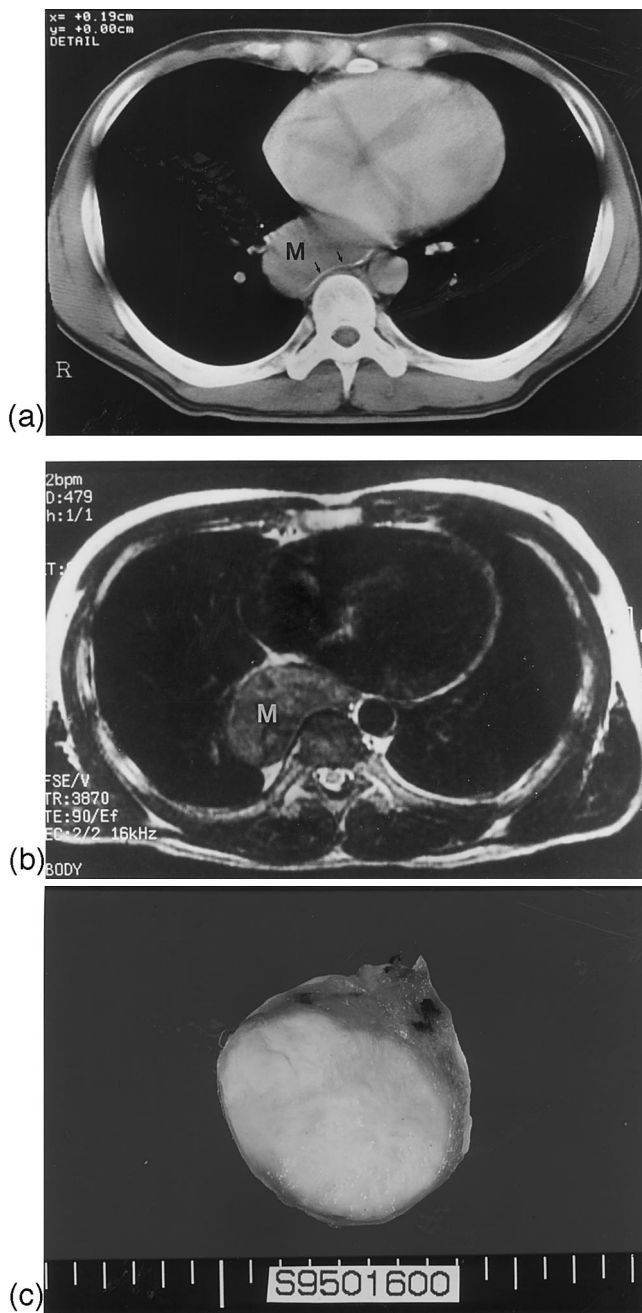


Fig. 13. Esophageal leiomyoma in a 35-year-old man. (A) Enhanced CT scan shows well-defined round mass (M) lateral to aorta. Widened gastrograffin filled esophageal lumen (arrows) is observed. (B) T2-weighted MR image shows mass (M) with low signal intensity. (C) Gross pathologic specimen shows a clearly defined tumor with light pink and whorled cut surface.

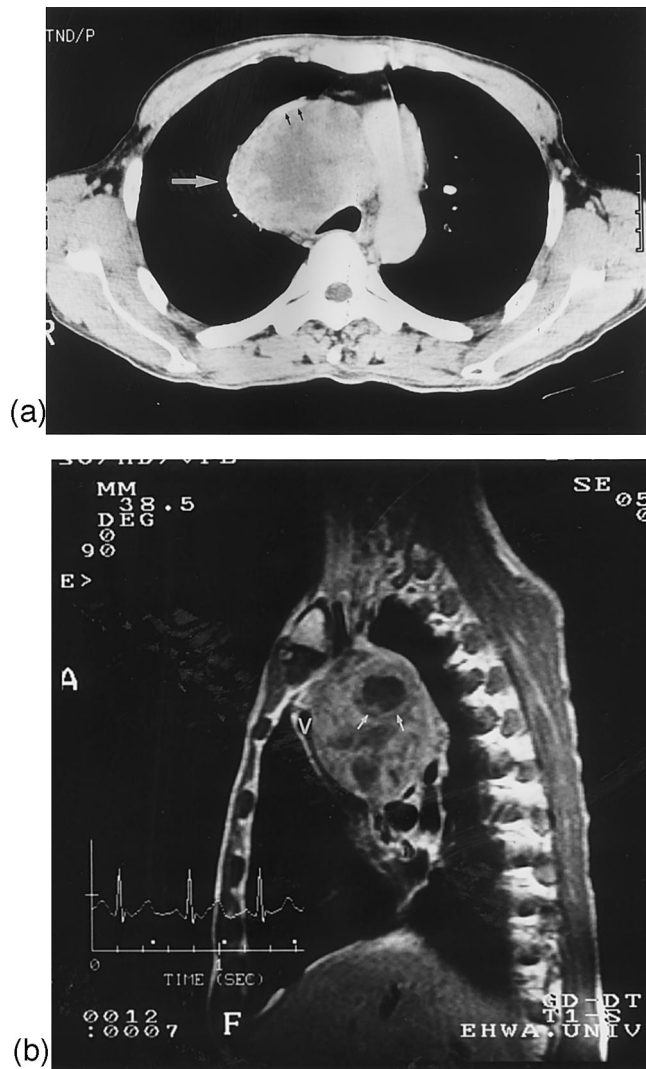


Fig. 14. Ectopic thymic carcinoma in a 54-year-old man. (A) Enhanced CT scan shows large mass (large arrow) with heterogeneous attenuation posterior to superior vena cava (small arrows). (B) Gadolinium-enhanced T1-weighted sagittal MR image shows mass containing low signal-intensity area (arrows), suggesting cystic change. V, superior vena cava.

on chest radiograph and CT [26] (Fig. 15). Accompanying pleural effusions are common.

3.6.2. Hemorrhage

Trauma to the aorta or its major branches is a common cause of mediastinal hemorrhage. At CT, streaky soft tissue attenuation is seen interspersed through the mediastinal fat. High attenuation associated with fresh thrombus can be seen on unenhanced CT scans (Fig. 16).

3.6.3. Aortic aneurysm or other abnormalities

Traumatic pseudoaneurysm usually arises from distal arch or upper descending aorta close to the ligamentum arteriosum (Fig. 16) [27]. Chronic traumatic pseudoaneurysm is saccular in shape and may develop calcification in the wall or lining thrombus.

3.6.4. Hernia

Hiatal hernia is a frequent incidental finding and produces a smooth focal mass with or without air or air-fluid level on chest radiograph. CT findings of herniated stomach with air in the lumen and surrounding fat suggest the diagnosis (Fig. 17).

3.6.5. Fibrosing mediastinitis

The most common cause of fibrosing mediastinitis is histoplasmosis, followed by tuberculosis, syphilis, and drug or radiation therapy. An idiopathic form is also reported. Dense fibrosis progressively encases and eventually obliterates the lumen of the mediastinal vessels and airways. Pulmonary oligemia resulting from bronchial, venous, or lymphatic obstruction or pleuropulmonary scarring may be seen [28] (Fig. 18).

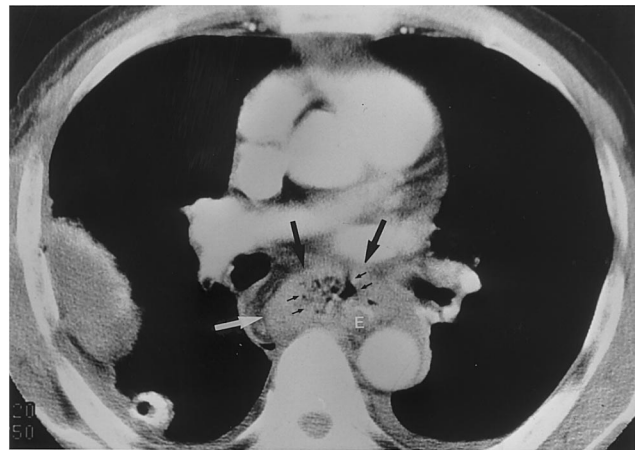


Fig. 15. Mediastinal abscess caused by esophageal perforation in a 56-year-old man. Enhanced CT scan shows fluid collection (large arrows) with air-bubbles (small arrows) in mediastinum and bilateral pleural effusion. Gastrografin filled esophagus (E) is observed.

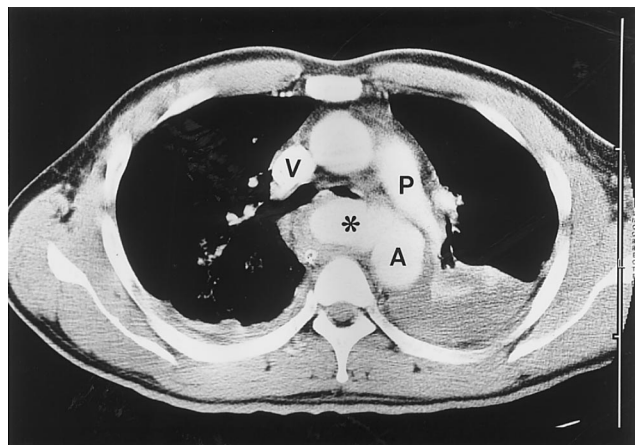


Fig. 16. Traumatic pseudoaneurysm of aorta with mediastinal hematoma in a 25-year-old man. Enhanced CT scan shows saccular projection (asterisks) from descending thoracic aorta (A) with high attenuation, suggesting pseudoaneurysm. P, pulmonary artery; V, superior vena cava.

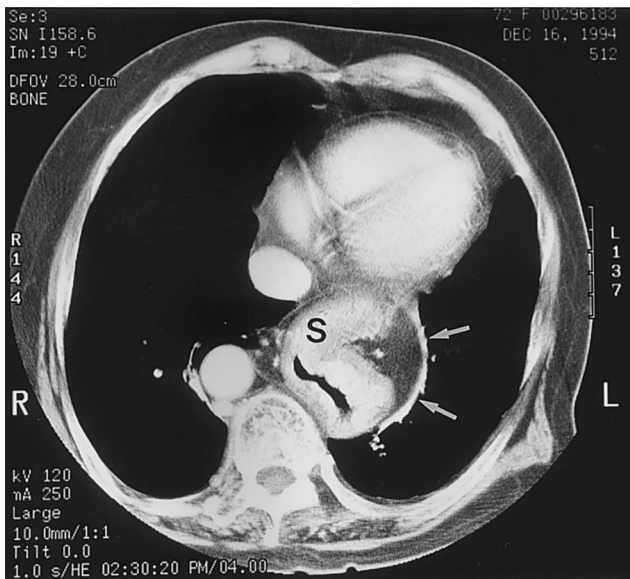


Fig. 17. Hiatal hernia in a 72-year-old woman. Contrast-enhanced CT scan shows elevated stomach (S) and surrounding fat (arrows).

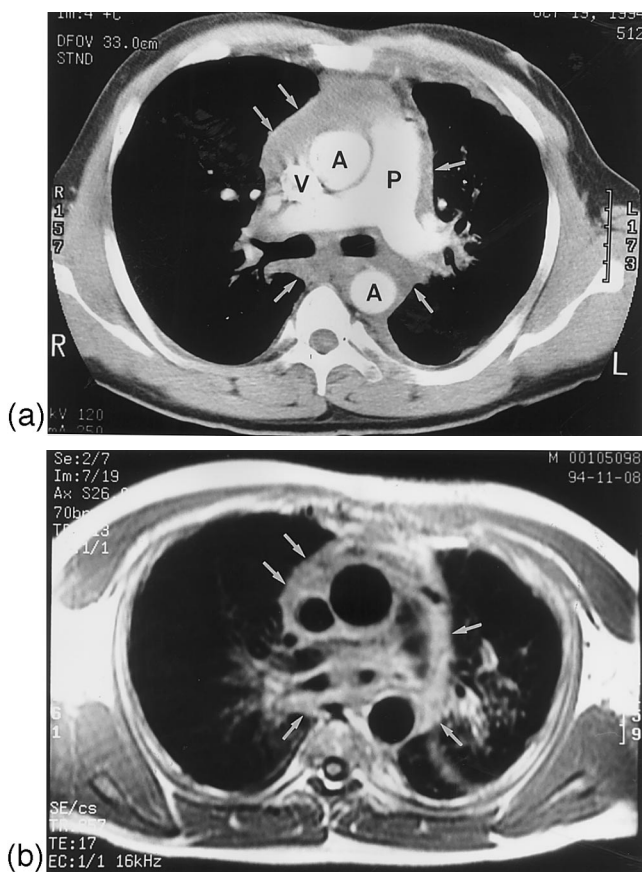


Fig. 18. Fibrosing mediastinitis in a 43-year-old man. (A) Contrast-enhanced CT scan and (B) T1-weighted MR image show infiltrating soft tissue mass (arrows) in mediastinum, encasing major vessels and airways. A, aorta; P, pulmonary artery; V, superior vena cava.

References

- [1] Felson B. Chest Roentgenology. Philadelphia, PA: Saunders, 1973:389–420.
- [2] Armstrong P. Neoplasms of the lungs, airways, and pleura. In: Armstrong P, Wilson AG, Dee P, Hansel DM, editors. Imaging of Diseases of the Chest. St. Louis, MO: Mosby, 1995:272–368.
- [3] Hopper KD, Diehl LF, Cole BA, Lynch JC, Meilstrup JW, McCauslin MA. Significance of necrotic mediastinal lymph nodes on CT in patients with newly diagnosed Hodgkin disease. *Am J Roentgenol* 1990;155:267–70.
- [4] Negendank WG, Al-Katib AM, Karanes C, Smith MR. Lymphomas: MR imaging contrast characteristics with clinicopathologic correlations. *Radiology* 1990;177:209–16.
- [5] Glazer HS, Molina PL, Siegel MJ, Sagel SS. High-attenuation mediastinal masses on unenhanced CT. *Am J Roentgenol* 1991;156:45–50.
- [6] Pitchenik AE, Fertel D, Bloch AB. Mycobacterial disease: epidemiology, diagnosis, treatment and prevention. *Clin Chest Med* 1998;8:425–41.
- [7] Im JG, Song KS, Kang HS, Yeon KM, Han MC, Kim CW. Mediastinal tuberculous lymphadenitis: CT manifestations. *Radiology* 1987;164:115–9.
- [8] McAdams HP, Rosado-de-Christenson M, Fishback NF, Templeton PA. Castleman disease of the thorax: radiologic features with clinical and histopathologic correlation. *Radiology* 1998;209:221–8.
- [9] Mendelson DS, Rose JS, Efremidis SC, Kirschner PA, Cohen BA. Bronchogenic cysts with high CT numbers. *Am J Roentgenol* 1983;140:463–5.
- [10] Naidich DP, Rumancik WM, Ettenger NA, Feiner HD, Harnanz-Schulman M, Spatz EM, Toder ST, Genieser WB. Congenital anomalies of the lungs in adults: MR diagnosis. *Am J Roentgenol* 1988;151:13–9.
- [11] Kuhlman JE, Fishman EK, Wang KP, Siegelman SS. Esophageal duplication cyst: CT and transesophageal needle aspiration. *Am J Roentgenol* 1985;145:531–2.
- [12] Wittich GR, Karnel F, Schurawitzki H, Jantsch H. Percutaneous drainage of mediastinal pseudocysts. *Radiology* 1988;167:51–3.
- [13] Dabir RR, Piccione W Jr, Kittle CF. Intrathoracic tumors of the vagus nerve. *Ann Thorac Surg* 1990;50:494–7.
- [14] Cohen LM, Schwartz AM, Rockoff SD. Benign schwannomas: pathologic basis for CT inhomogeneities. *Am J Roentgenol* 1986;147:141–3.
- [15] Sakai F, Sone S, Kiyono K, Maruyama A, Ueda H, Aoki J, Kawai T, Ishii K, Morimoto M, Huniuda M, Koizumi T. Intrathoracic neurogenic tumors: MR-pathologic correlation. *Am J Roentgenol* 1992;159:279–83.
- [16] Reed JC, Haller KK, Feigin DS. Neural tumors of the thorax: subject review from the AFIP. *Radiology* 1978;126:9–17.
- [17] Olsen WL, Dillon WP, Kelly WM, Norman D, Brant-Zawadzki M, Newton TH. MR imaging of paragangliomas. *Am J Roentgenol* 1987;148:201–4.
- [18] Spizarny DL, Rebner M, Gross BH. CT evaluation of enhancing mediastinal masses. *J Comput Assist Tomogr* 1987;11:990–3.
- [19] Kline ME, Patel BU, Agosti S. Non-infiltrating angioliopoma of the mediastinum. *Radiology* 1990;175:737–8.
- [20] Shatter K, Rosado-de-Christenson ML, Patz EF Jr, Young S, Farver CF. Thoracic lymphoangioma in adults: CT and MR imaging features. *Am J Roentgenol* 1994;162:283–9.
- [21] Rietz KA, Werner B. Intrathoracic goitre. *Acta Chir Scan* 1960;119:379–402.
- [22] Bashist B, Ellis K, Gold RP. Computed tomography of intrathoracic goiter. *Am J Roentgenol* 1983;140:445–60.
- [23] Armstrong P. Mediastinal and hilar disorders. In: Armstrong P, Wilson AG, Dee P, Hansel DM, editors. Imaging of Diseases of the Chest. St. Louis, MO: Mosby, 1995:717–816.

- [24] Tan A, Holdener GP, Hecht A, Gelfand C, Baker B. Malignant thymoma in an ectopic thymus: CT appearance. *J Comput Assist Tomogr* 1991;15:842–4.
- [25] Lewis JE, Wick MR, Scheithauer BW, Bernatz PE, Taylor WF. Thymoma: a clinicopathological review. *Cancer* 1987;60:2727–43.
- [26] Carrol CL, Jeffrey RB, Federle MP, Vernacchia FS. CT evaluation of mediastinal infections. *J Comput Assist Tomogr* 1989;11:449–54.
- [27] Lundell CJ, Quinn M, Rinck E. Traumatic laceration of the ascending aorta: angiographic assessment. *Am J Roentgenol* 1985;145:715–9.
- [28] Weinstein JB, Aronberg DJ, Sagel SS. CT of fibrosing mediastinitis: findings and their utility. *Am J Roentgenol* 1983;141:247–51.